IONIZING RADIATION CALCULATIONS AND COMPARISONS WITH LDEF DATA*

T. W. Armstrong and B. L. Colborn
Science Applications International Corporation
Route 2, Prospect, TN 38477
Phone: 615/468-2603, Fax: 615/468-2676

J. W. Watts, Jr.
ES62, NASA/Marshall Space Flight Center, AL 35812
Phone: 205/544-7693, Fax: 205/544-7754

SUMMARY

In conjunction with the analysis of LDEF ionizing radiation dosimetry data, a calculational program is in progress to aid in data interpretation and to assess the accuracy of current radiation models for future mission applications. To estimate the ionizing radiation environment at the LDEF dosimeter locations, scoping calculations for a simplified (one-dimensional) LDEF mass model have been made of the primary and secondary radiations produced as a function of shielding thickness due to trapped proton, galactic proton, and atmospheric (neutron and proton cosmic-ray albedo) exposures. Preliminary comparisons of predictions with LDEF induced radioactivity and dose measurements have been made to test a recently developed model of trapped proton anisotropy.

INTRODUCTION

Purpose

A calculational program is in progress as part of the LDEF ionizing radiation investigations, with the following objectives:

Data Analysis Support - Calculations are being used to help interpret the LDEF ionizing radiation measurements. In most cases the LDEF dosimetry data represent an integration of several effects, such as contributions from different environment sources (galactic and trapped radiation), influence of shielding variations (from both experimental apparatus and spacecraft structure), and secondary particle contributions from nuclear interactions. The calculations can be used to "unfold" the dosimetry data to estimate the influence of these individual effects, which is needed if the LDEF data are to be fully applicable for future missions having different orbit parameters and spacecraft configurations.

Model Validation - LDEF data are being utilized to evaluate the accuracy of present ionizing radiation models. This includes models for predicting both the "external" environments (ionizing radiation fields external to the spacecraft) and the "internal" environments (ionizing radiation environments at locations internal to the spacecraft, which include the effects of radiation interactions and transport).

*Work partially supported by NASA Marshall Space Flight Center, Huntsville, AL, Contract NAS8-38566.

Future Mission Applications - The overall objective of the calculational program is to fully utilize the LDEF data to test and revise current ionizing radiation models for future mission applications. This should result in more accurate models for predicting crew dose for planned long duration missions (Space Station Freedom, Space Exploration Initiative) and for assessing radiation backgrounds to sensors and determining achievable measurement sensitivities for planned space-based observatories (e.g., Earth Observing Observatory). Furthermore, benchmarking models with LDEF data will reduce present model uncertainties involved in assigning hardware design margins for meeting mission radiation requirements. This will help prevent both "under-design" (which can lead to reduced mission performance) and "over-design" (resulting in excessive costs).

LDEF Data for Radiation Model Validation

The LDEF mission had several unique features that are important to the validation of ionizing radiation models:

Well Instrumented - A variety of different types of radiation dosimetry, with multiple dosimeters of each type,were onboard, providing a high-confidence data set for benchmarking the models. Also, dosimeters were placed at various locations on the spacecraft and behind various thicknesses of shielding, allowing tests of both external environment models and the transport models for predicting the radiation environment internal to the spacecraft.

Long Exposure - Dosimetry results have high statistical accuracy due to the long mission duration. This is particularly important for checking model predictions of the high-LET component of cosmic rays and nuclear interaction products, which is of key importance in assessing radiation-induced biological and electronics damage.

Fixed Orientation - The very stable orientation of LDEF during the entire mission ($< 0.2°$, ref. 1), together with dosimetry placements at various positions around the spacecraft, allow the directionality of the incident radiation to be measured. This provides a unique opportunity for testing a recently-developed model (ref. 2) for predicting the directionality of the trapped proton flux. Since the radiation dose (at most shielding depths) for spacecraft in low-earth orbit is dominated by the trapped proton exposure, this anisotropy may have practical importance for planned fixed-orientation spacecraft in low-earth orbit, such as for Space Station Freedom.

Thus, the LDEF data provide a significant opportunity for model improvement in addressing ionizing radiation issues for future missions, as summarized in figure 1.

APPROACH

Figure 2 gives an overview of the calculational approach and indicates some of the specific models being used. External environment models include the AP8 and AE8 models for trapped protons and electrons (refs. 3,4), the MSFC model for predicting trapped proton anisotropy (ref. 2), and the galactic proton and heavy ion environments given by the NRL CREME model (ref. 5). Transport models include both simplified, one-dimensional models commonly used in quick assessments of space radiation effects -- the MSFC analytical models for proton and electron-bremsstrahlung transport (refs. 6,7), SHIELDOSE (ref. 8), and CREME (ref. 5) -- as well as three-dimensional Monte Carlo codes, HETC (ref. 9) and MORSE (ref. 10). The Monte Carlo codes take into account in detail the secondary particle production and transport and can treat three-dimensional, multimedia spacecraft models, capabilities which are needed in some cases for definitive comparisons with the LDEF measurements.

This calculational approach can provide predictions for all of the different types of LDEF radiation measurements - namely: (a) induced radioactivity, including both the activation of metal samples (Ni, Co, V, Ta, and In) placed in LDEF experiment packages and the activation of various spacecraft structural components (e.g., trunnions, experiment tray clamps); (b) measurements of tissue-equivalent absorbed dose using thermoluminescence detectors (TLDs); (c) measurements of linear-energy-transfer (LET) spectra by plastic nuclear track detectors (PNTDs); and (d) particle fluence and energy spectra, including secondary neutrons, as measured by fission foils, specific activation reactions, low-energy neutron detectors (^{6}LiF foils), and PNTDs.

The shaded areas in figure 2 indicate the emphasis of the modeling to date. An important approximation for the initial calculations is that a very simplified (in most cases one-dimensional) spacecraft model has been used. To obtain definitive comparisons with most of the measurements, detailed shielding variations about the detector need to be taken into account, so development of a 3-D LDEF mass model for radiation calculations is underway (ref. 11).

RESULTS

Emphasis of the initial calculations has been in two areas: (a) scoping calculations of the importance of different exposure sources and secondary particles to the induced radiation environment, and (b) calculations and comparisons with measurements to check the accuracy of a recent model for predicting the anisotropy of trapped protons.

Scoping Calculations

The penetrating radiation environment for the LDEF orbit consisted of protons (with a relatively small contribution of heavier ions) trapped in the earth's magnetic field, protons and heavier ions of galactic origin, and albedo neutrons and protons due to galactic cosmic-ray bombardment of the earth's atmosphere (ref. 12). Since the angular variation of these sources is quite different (figure 3), and since material attenuation within LDEF is different for each source, an important question for data interpretation concerns the magnitude of the contribution from each component at the LDEF measurement locations. Thus, a set of scoping calculations was made to obtain a general indication of (a) the importance of different space radiation sources, (b) the importance of secondary particles generated within LDEF, and (c) the spatial variation of the induced radiation environment.

The calculations were carried out using Monte Carlo transport methods, with the SAIC version of the HETC code (ref. 13) for high-energy transport and the MORSE code for low-energy (< 20 MeV) neutron transport. These were only scoping estimates because several important approximations have been made in this initial work -- e.g., a one-dimensional (aluminum slab) model of LDEF was used, and the angular variation of the incident radiation (particularly the trapped proton anisotropy) was not accurately simulated. Subsequent calculations using a 3-D LDEF mass model are planned to remove these approximations.

Example results are shown in figure 4 for the depth-dependent particle fluence, and figure 5 shows fluence spectra at a particular depth (10 g/cm^2). (To roughly relate these depths in terms of areal density to LDEF, if the LDEF spacecraft is represented as a cylinder the average areal density is 32 g/cm^2 across the diameter and and 68 g/cm^2 end to end.) These results indicate that the contribution from albedo neutrons and protons is negligible, and that the relative importance of

trapped vs. galactic sources depends on the shielding depth and radiation effect of interest. In terms of fluence over all energies, figure 5 shows that secondary neutrons dominate for depths $\gtrsim 10$ g/cm^2.

A report on additional results from these calculations, including the induced radioactivity in aluminum and stainless steel produced by different sources and particle types, is available (ref. 14), and a summary has been accepted for journal publication (ref. 15).

Trapped Proton Anisotropy

The ionizing radiation dose at most shielding depths for spacecraft in low-earth orbit (LEO) is produced mainly by trapped protons in the South Atlantic Anomaly (SAA) region. The standard NASA models (AP8MIN and AP8MAX) for describing the trapped proton environment do not provide an angular dependence, although the proton flux is actually highly anisotropic in the SAA. This anisotropy has not been an important practical consideration for most previous LEO missions because the varying spacecraft attitude during passage through the radiation belt "averages out" anisotropic effects over many orbits. However, for the fixed orientation of LDEF, and for several planned missions (e.g., Space Station Freedom, Earth Observing Satellite) where the spacecraft will be gravity-gradient stabilized, the cumulative proton exposure will remain anisotropic, and will result in a highly nonuniform dose distribution around the spacecraft.

Watts, et al. (ref. 2) have recently developed a model to predict orbit-average, angular dependent trapped proton flux spectra from the standard omnidirectional AP8MIN and AP8MAX data bases. Since trapped proton anisotropy effects may be an important consideration for Space Station design and operation, a priority for the calculational work has been to utilize LDEF data to evaluate the accuracy of this anisotropy model, as summarized below. These initial results must be considered as preliminary because of several simplifications in the calculations to date, and because the LDEF data are not yet fully analyzed.

Anisotropy of Tray Clamp Activation

The measured induced radioactivity of the aluminum clamps (ref. 16) used to secure the LDEF experiment trays provides very appropriate data for checking the anisotropy model since these clamps are located on all sides of the spacecraft and at various directions relative to the flight vector. Also, since the clamps are located on the outer surface and are thin (1.3 g/cm^2), we expect (based on the scoping Monte Carlo calculations; e.g., figure 4) the activation from galactic protons and secondary particles to be small, so the measured activation is predominantly from the primary trapped protons.

The ^{22}Na production in aluminum has been predicted as a function of direction (in the horizontal plane perpendicular to the LDEF longitudinal axis) and for various shielding depths (figure 6). These calculations were made for a point behind an aluminum slab shield (assuming that the direction normal to the plane is pointed in the plotted direction, and assuming that no particles enter from the "back side" of the plane). The proton transport code of Burrell (ref. 6) was used. The angular distribution of the trapped protons were taken from a pre-computed data base for discrete altitudes (ref. 17), with results for 450 km and solar minimum used here; thus, the properly averaged angular spectra for solar cycle variation and the varying altitudes during the LDEF mission have not yet been applied.

The results (figure 6) show minimum activation near the East (leading edge) of the spacecraft and maximum activation near the West (trailing) direction. The predicted anisotropy in terms of the ratio of West-side activation to East-side activation varies from a factor of about 1.8 near the surface to a factor of 3.5 at 10 g/cm^2 depth. This increase in anisotropy with depth is due to the increasing anisotropy of the incident protons at higher energies (refs. 2, 18).

A comparison of the predicted ^{22}Na activation at a depth corresponding to the mid-depth of the tray clamp (0.64 g/cm^2) with the measured activation (ref. 16) is shown in fig. 7, indicating very good agreement for these preliminary comparisons. The angular variations are similar in shape, with the maximum/minimum ratio with respect to direction being 1.8 for the measurements vs. 2.0 for the calculations.

The calculated results in figure 7 are lower than the measurements by about 15% for directions in the vicinity of West, and lower by about 50% for directions near East. These preliminary absolute magnitude comparisons suggest a better accuracy for the AP8 trapped proton model than the factor of two uncertainty commonly quoted.

Dose Anisotropy

Predictions of the absorbed dose anisotropy have also been made and compared with the initial TLD measurements reported by Benton, et al. (ref. 19) for Experiments P0006 (bay-row location F-2, near the trailing edge) and M0004 (tray position F-8, near leading edge). These initial calculations were also made assuming one-dimensional, plane-geometry shielding, so the results are preliminary.

The predicted ratios are compared with the measured P0006-to-M0004 TLD dose ratios (using data from ref. 18 with interpolation applied to obtain common shielding depths) in figure 8. These preliminary comparisons also indicate that the anisotropy model predictions are consistent with LDEF data.

Directionality of Trunnion Activation

The measured spatial dependence of radioisotopes produced in the stainless steel LDEF trunnions (refs. 20, 21) also provide an opportunity for checking the anisotropy model. To date, calculations have been made to compare with only a small subset of the measured data, with some initial comparisons for the ^{54}Mn activity given here.

The calculations were made for a "simplified" 3-D geometry with the body of the LDEF spacecraft and experiment trays modeled as a homogeneous aluminum cylinder (with an average density to preserve the total mass), and with the earth-end trunnion represented as a stainless steel rod. The activation at a point in the trunnion was computed by (a) determining the areal density along a 3-D grid of rays emanating from the point (720 rays were used, corresponding to the polar-azimuthal angular grid used in generating the directional proton environment), (b) computing the attenuation for each ray using the Burrell 1-D proton transport code, with solid-angle weighting for each ray to get the cumulative proton spectrum at the point, and (c) folding this spectrum with cross sections for ^{54}Mn production from the constituents of stainless steel.

Shown in figure 9 is a comparison of the calculational results with the measurements of Moss and Reedy (ref. 20) for the radial distribution of ^{54}Mn produced in a section of the trunnion centered 3.5 in. from the end ("Section D" in fig. 8a of ref. 20) of the East (leading edge)

trunnion. These results are for two angular segments of the trunnion having surface normals pointed in the zenith direction (labeled "space") and toward the center of the earth (labeled "earth"). The trapped proton anisotropy model predicts that the external fluxes directed toward the "space" and "earth" directions should be essentially the same, whereas the measurements and transport calculation results indicate a lower activation in the space direction. A separate calculation made with only the trunnion present shows that the lower activation observed in the space direction is due to the shielding effect of the LDEF spacecraft.

The agreement between the predicted and measured activations in figure 9 is quite good near the surface of the trunnion, but the agreement becomes somewhat worse near the center. Results from the 1-D Monte Carlo calculations (ref. 14) show that galactic protons contribute substantially at penetration depths comparable to the center of the trunnion. Thus, the underprediction of the activation deep into the trunnion indicated in figure 9 may be due to the neglect of incident galactic protons in these initial calculations.

CONCLUSIONS

LDEF has provided unique data which, based on preliminary comparisons of initial measurements and predictions, confirms a recently developed model for the anisotropy of trapped protons. This anisotropy is important in predicting the radiation exposure of other fixed-orientation spacecraft in LEO, such as the planned Space Station and Earth Observing Satellite missions.

Preliminary comparisons also indicate that the LDEF radiation dosimetry data are in good agreement with predictions using AP8 trapped proton flux model. Such results can help quantify the limits on safety margins commonly applied to account for radiation environment modeling uncertainties in spacecraft design and parts selection and in crew dose assessments.

The emphasis of near-term future calculations is expected to be on model comparisons with LDEF LET measurements (e.g., ref. 22). LET spectra generally provide a more stringent test of the environment and transport models than considered to date for induced radioactivity and dose comparisons, and LET is fundamental in assessing electronics upsets and biological damage. For future calculations a three-dimensional LDEF geometry/mass model will be implemented to properly account for dosimetry shielding effects and provide more definitive assessments of the radiation models.

REFERENCES

1. Gregory, J. C. and Peters, P. N.: LDEF Attitude Measurements Using a Pinhole Camera with a Silver/Oxygen Atom Detector. Initial Results. First LDEF Post-Retrieval Symposium. NASA CP- 3134, 1992.

2. Watts, J. W., Jr.; Parnell, T. A. and Heckman, H. H.: Approximate Angular Distribution and Spectra for Geomagnetically Trapped Protons in Low-Earth Orbit. A. C. Rester, Jr., and J. I. Trombka (Eds.), AIP Conf. Proc., New York, 1989.

3. Sawyer, Donald M. and Vette, James I.: AP8 Trapped Proton Environment for Solar Maximum and Solar Minimum. National Science Data Center, Goddard Space Flight Center, NSSDC/WDC-A-R&S 76-06, 1976.

4. Teague, Michael, J.; Chan, King, W. and Vette, James I.: AE6: A Model Environment of the Trapped Electrons for Solar Maximum. National Science Data Center, Goddard Space Flight Center, NSSDC/WDC-A-R&S 76-04, 1976.

5. Adams, James: Cosmic Ray Effects on MicroElectronics, Part IV. NRL Memorandum Report 5901, December 31, 1986.

6. Burrell, Martin O.: The Calculation of Proton Penetration and Dose Rates. Marshall Space Flight Center, NASA TM X-53063, 1964.

7. Watts, John W., Jr. and Burrell, M. O.: Electron and Bremsstrahlung Penetration and Dose Calculation. National Aeronautics and Space Administration, NASA TN D-6385, 1971.

8. Seltzer, Stephen: SHIELDOSE: A Computer Code for Space-Shielding Radiation Dose Calculations. National Bureau of Standards Technical Note 1116, May 1980.

9. Armstrong, T. W. and Chandler, K. C.: The High-Energy Transport Code HETC. Nucl. Sci. Engr. 49, 110 (1972).

10. Straker, E. A.; Stevens, P. N.; Irving, D. C. and Cain, V. R.: The MORSE Code - A Multigroup Neutron and Gamma-Ray Monte Carlo Transport Code. ORNL-4585, September 1970.

12. Watts, J. W.,Jr.; Parnell, T. A.; Derrickson, James H.; Armstrong, T. W. and Benton, E. V.: Prediction of LDEF Ionizing Radiation Environment. First LDEF Post-Retrieval Symposium. NASA CP-3134, 1992.

11. Colborn, B. L. and Armstrong, T. W.: LDEF Geometry/Mass Model for Radiation Analyses. Radiation Exposure of LDEF: Initial Results. First LDEF Post-Retrieval Symposium. NASA CP-3134, 1992.

13. Armstrong, T. W. and Colborn, B. L.: A Thick-Target Radiation Transport Code for Low Mass Heavy Ion Beams, HETC/LHI. Nucl. Instr. Meth. 169, 161 (1980).

14. Armstrong, T. W. and Colborn, B. L.: Scoping Estimates of the LDEF Satellite Induced Radioactivity. Science Applications International Corporation Report SAIC-90/1462, September 1990.

15. Armstrong, T. W. and Colborn, B. L.: Predictions of Induced Radioactivity for Spacecraft in Low-Earth Orbit, accepted for publication in Radiation Measurements.

16. Harmon, B. A.; Fishman, G. J.; Parnell, T. A. and Laird, C. E.: LDEF Induced Radioactivity Analysis. First LDEF Post-Retrieval Symposium. NASA CP-3134, 1992.

17. Colborn, B. L.; Armstrong, T. W. and Watts, J. W. Jr.: Data Base Description and Retrieval Program for the Trapped Proton Vector Flux Data Bases VF1MIN and VF1MAX. Science Applications International Corporation Report SAIC-90/1475, October 1990.

18. Armstrong, T. W.; Colborn, B. L. and Watts, J. W. Jr.: Characteristics of Trapped Proton Anisotropy at Space Station Freedom Altitudes. Science Applications International Corporation SAIC-90/1474, October 1990.

19. Benton, E. V.; Frank, A. L.; Benton, E. R.; Csige, I.; Parnell, T. A. and Watts, J. W., Jr.: Radiation Exposure of LDEF: Initial Results. First LDEF Post-Retrieval Symposium. NASA CP-3134, 1992.

20. Moss, Calvin E. and Reedy, Robert C.: Measurements of Induced Radioactivity in Some LDEF Samples. First LDEF Post-Retrieval Symposium. NASA CP-3134, 1992.

21. Winn, Willard G.: Gamma-Ray Spectrometry of LDEF Samples at SRL (U). First LDEF Post-Retrieval Symposium. NASA CP-3134, 1992.

22. Csige, I.; Benton, E. V.; Frank, A. L.; Frigo, L. A.; Benton, E. R.; Parnell, T. A., and Watts, J. W., Jr.: Charged Particle LET-Spectra Measurements Aboard LDEF. First LDEF Post-Retrieval Symposium. NASA CP-3134, 1992.

Unique Features of LDEF Mission	Importance to Ionizing Radiation Data Collection	Importance to Model/Code Validation	Importance to Future LEO Missions
• Well-instrumented for ionizing radiation measurements	• Extensive radiation dosimetry: - *6 different types of dosimetry* - *multiple dosimeters of each type (≈ 200 TLD's, > 500 PNDT's, > 400 activation samples)* - *multiple dosimetry locations (in 16 different experimental trays)*	• Data sufficiently extensive and detailed to allow variety of modeling checks - e.g.: - *absorbed dose* - *proton and heavy ion fluence* - *energy spectra* - *LET spectra* - *secondary neutron fluence and spectra*	• Allows benchmarking and improvements of predictive methods for addressing ionizing radiation issues: - *dose to astronauts* - *electronics upset/burnout* - *materials damage* - *radiations backgrounds to sensitive instrumentation*
• Long mission duration	• High statistical accuracy of dosimetry results	• Unprecedented data accuracy for checking model predictions of high-LET radiation from high-Z cosmic rays and nuclear recoils	• High-LET radiation component is of key importance in assessing "single-hit" phenomena: - *biological effects* - *Single-Event-Upsets of electronics*
• Fixed orientation (< 0.2° wobble during mission)	• Allows measurement of trapped proton anisotropy	• Unprecedented data for testing models of trapped proton anisotropy	• Trapped proton anisotropy important for LEO, fixed-orientation spacecraft (such as Space Station Freedom, EOS)

Figure 1. Significance of LDEF data for validation of ionizing radiation models.

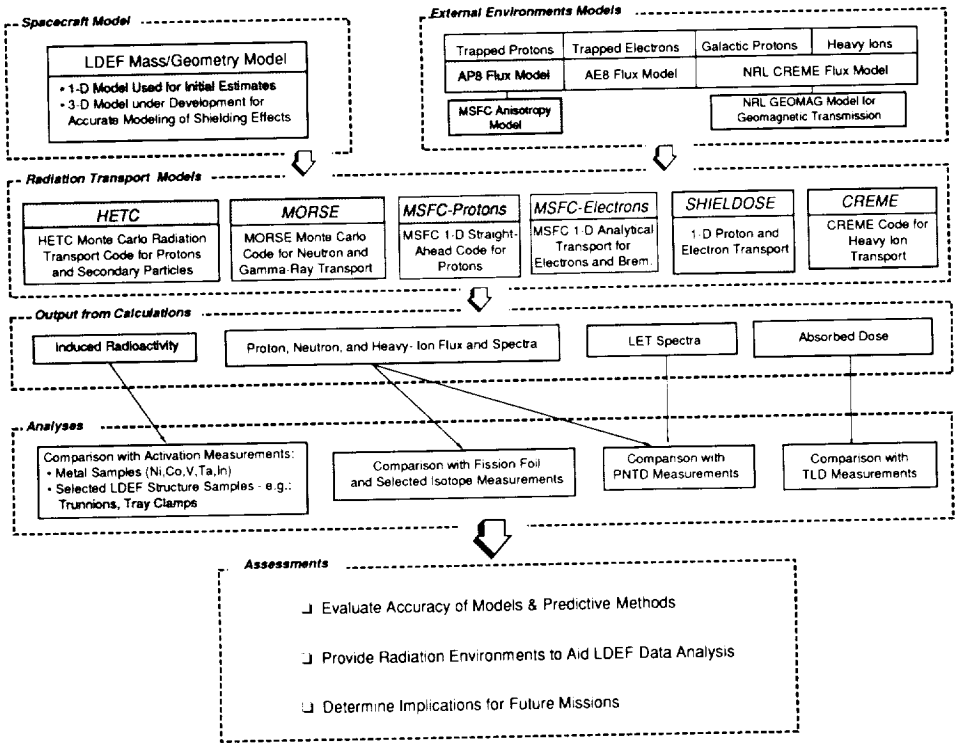

Figure 2. Overview of approach and models for LDEF ionizing radiation calculations.

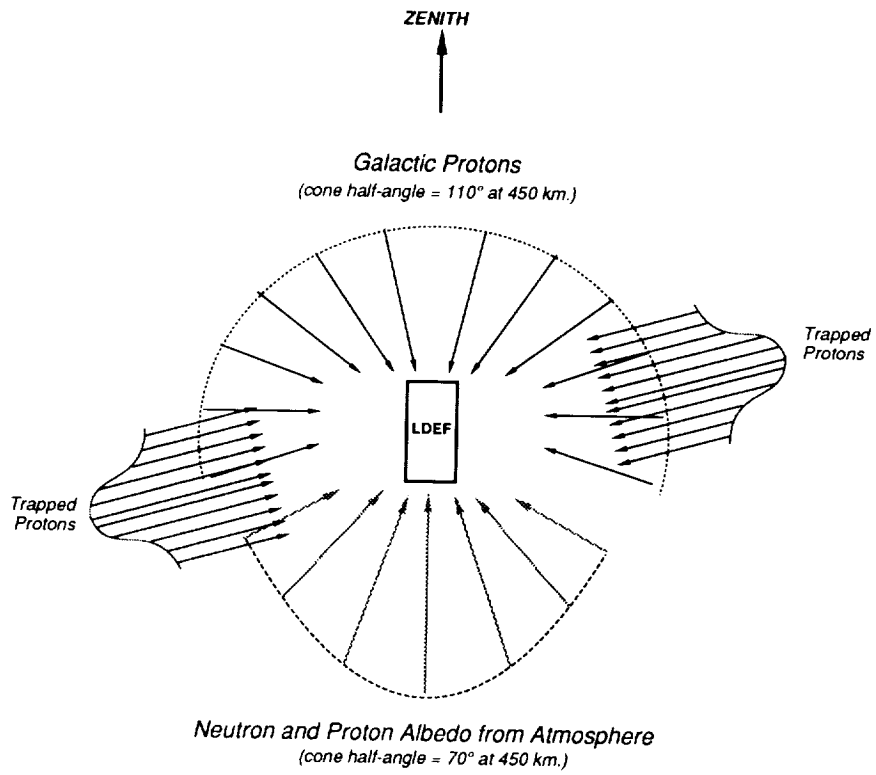

Figure 3. Illustration of the nonuniform angular variation of LDEF exposure to ionizing radiation.

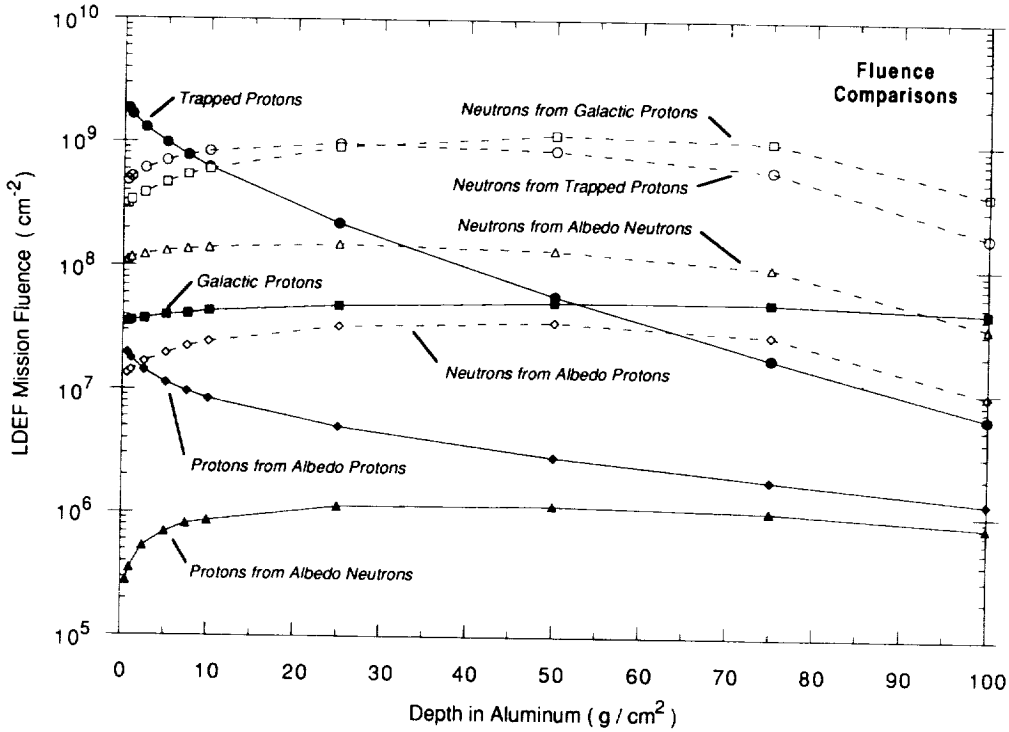

Figure 4. Predicted depth dependence of proton (primary and secondary) and neutron fluences over all energies produced by trapped proton, galactic proton, albedo proton, and albedo neutron environments over the duration of the LDEF mission. The different environments are all assumed incident isotropically on one side (0 depth) of an aluminum slab 100 g/cm2 in thickness.

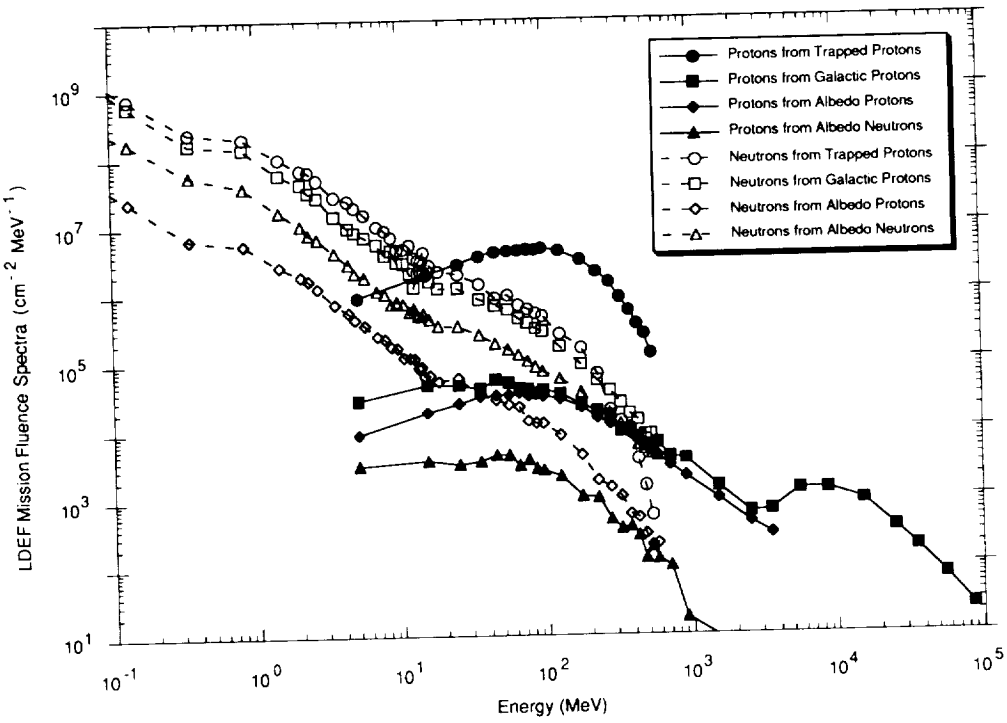

Figure 5. Comparison of predicted proton (primary and secondary) and neutron fluence at a depth of 10 g/cm^2 in aluminum from LDEF exposure to ionizing radiation sources.

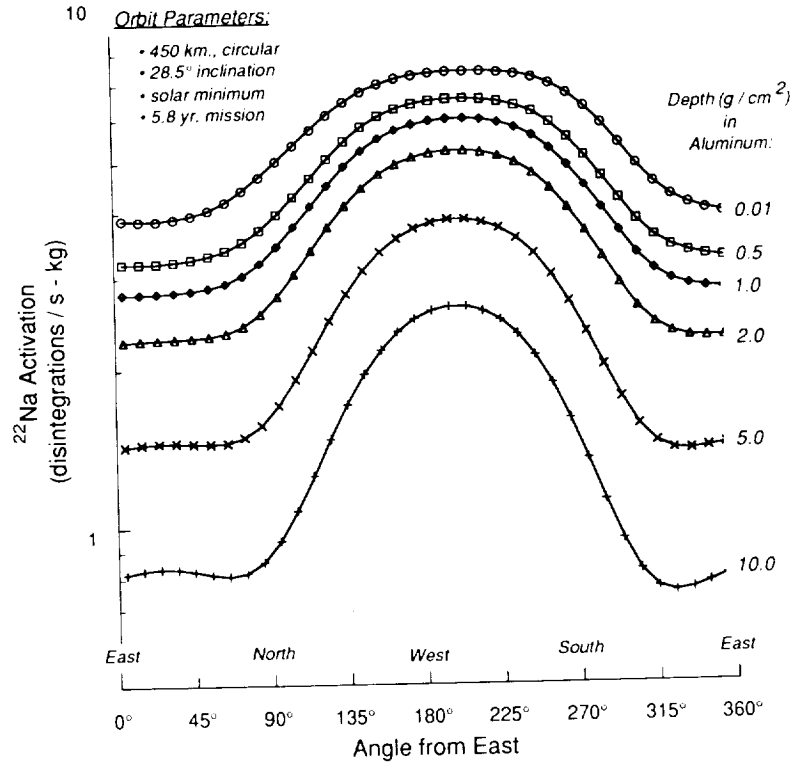

Figure 6. Predicted directionality of ^{22}Na production in aluminum due to trapped proton anisotropy.

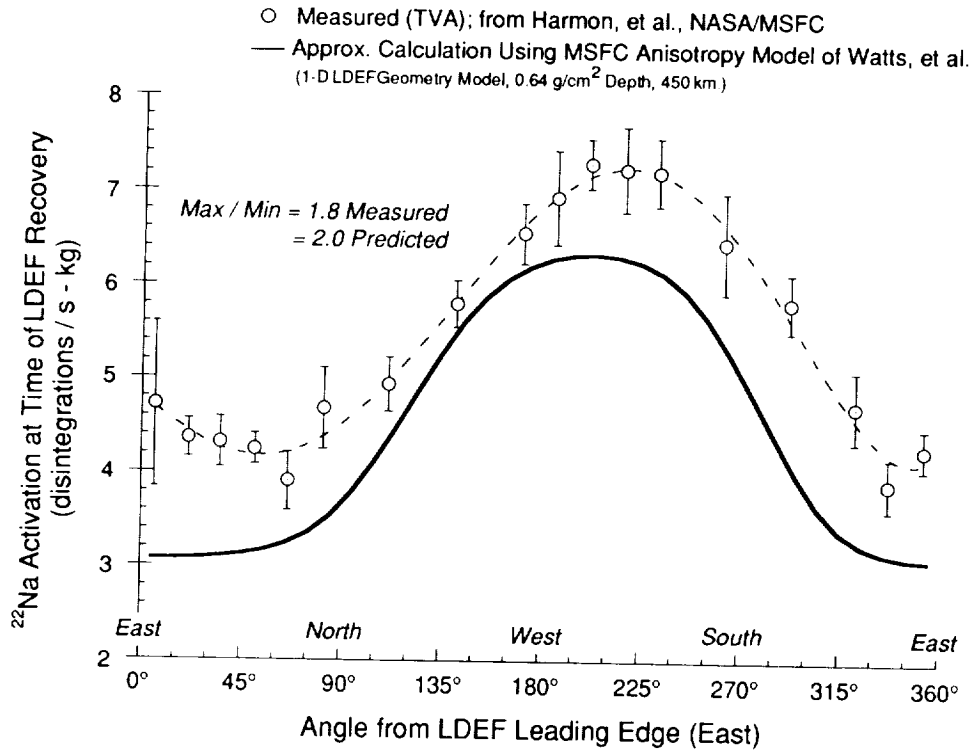

Figure 7. Preliminary comparison of predicted vs. measured (ref. 16) effects of trapped proton anisotropy in terms of ^{22}Na radioactivity induced in aluminum clamps of LDEF experiment trays.

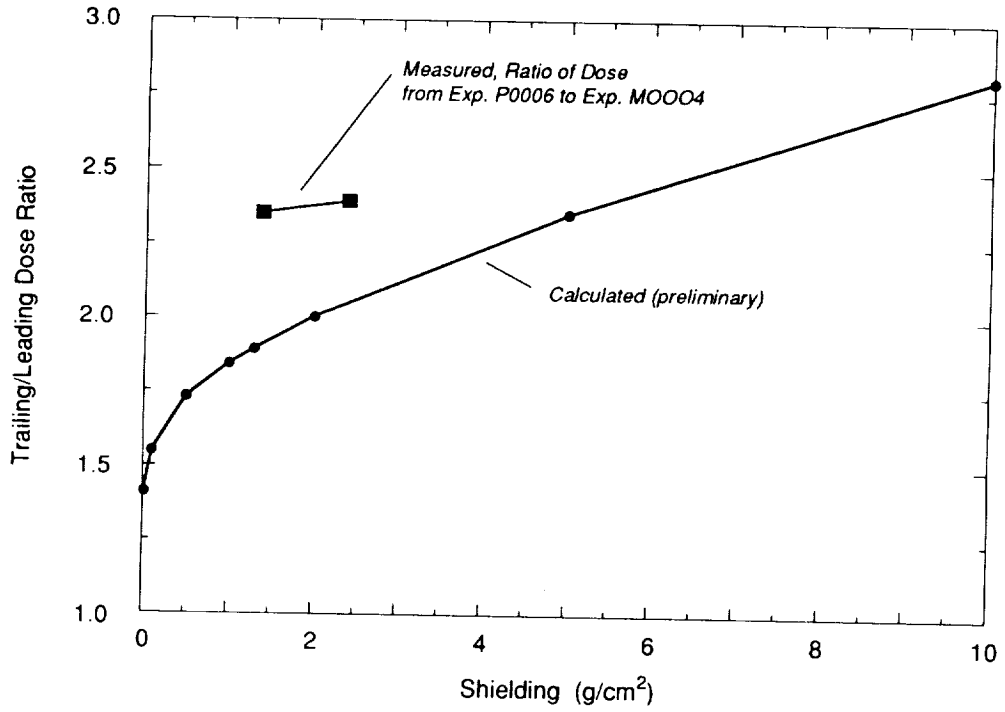

Figure 8. Calculated ratio of absorbed dose in tissue as function of shielding depth (aluminum equivalent) on trailing (West) vs. leading (East) side of LDEF compared with ratio from the TLD (thermoluminescent dosimetry) measurements of Experiments P0006 and M0004 (ref. 19)

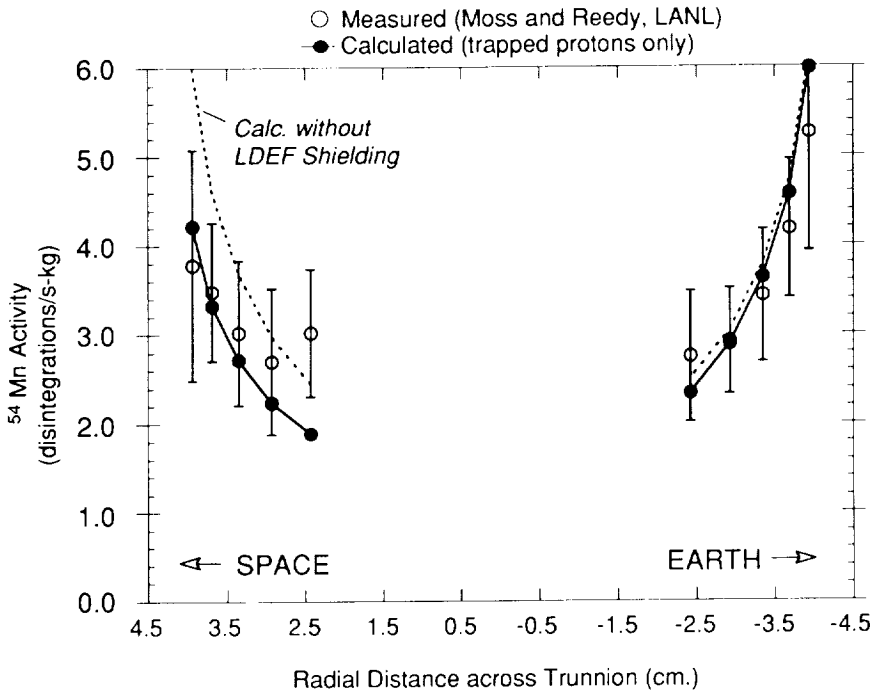

Figure 9. Comparison of calculated and measured (ref. 20) induced radioactivity in leading (East) LDEF trunnion. The solid curves were calculated with a geometry that included a mass representation of the LDEF spacecraft and the trunnion. For the dotted curves the spacecraft was removed.